P. Platania et al.

Optical Modelling and Physical Performances Evaluations for the JT-60SA ECRF Antenna

(27th April 2015 – 29th April 2015)
Lake Arrowhead, California, USA

Optical Modeling and Physical Performances Evaluations for the JT-60SA ECRF Antenna

P. Platania[1, a)] L. Figini[1], D. Farina[1], A. Isayama[2], T. Kobayashi[2], D. Micheletti[1], S. Moriyama[2], A. Moro[1] and C. Sozzi[1]

[1]*Istituto di Fisica del Plasma "P. Caldirola", Consiglio Nazionale delle Ricerche, Via R. Cozzi 53, 20125, Milano, Italy*
[2]*Japan Atomic Energy Agency, 801-1 Mukoyama, Naka, Ibaraki 311-0193, Japan*

[a)]Corresponding author: platania@ifp.cnr.it

Abstract. The purpose of this work is the optical modeling and physical performances evaluations of the JT-60SA ECRF launcher system. The beams have been simulated with the electromagnetic code GRASP® and used as input for ECCD calculations performed with the beam tracing code GRAY, capable of modeling propagation, absorption and current drive of an EC Gaussian beam with general astigmatism. Full details of the optical analysis has been taken into account to model the Gaussian beams. Inductive and advanced reference scenarios has been analysed for physical evaluations in the full poloidal and toroidal steering ranges for two slightly different layouts of the launcher system.

MODELING OF THE OPTICAL SYSTEM AND BEAM SIMULATIONS

In the JT-60SA tokamak four ECRF launchers will be installed and used for local heating, current drive and plasma initiation by injection of high-power and long-pulse EC waves into the plasma at 110 and 138 GHz. The requirements of a wide poloidal injection angle range together with a water cooling system with low risk of water leakage has driven a front steering antenna design including first mirrors with linear motion and a fixed second mirror. In the reference design ("baseline" hereafter) each antenna unit is composed by two corrugated waveguides (wg$_1$ and wg$_2$, aperture 60.3 mm) facing two identical flat mirrors M1 (dim. 400x500 mm) moving along an axis parallel to the waveguide and rotating around it [1] by means of a driving shaft. The beams are then reflected by a large fixed cylindrical mirror M2 (R_{cyl} = 0.7 m, dim. 400x500 mm) and directed towards the plasma through a rectangular aperture in the conducting shell for vertical stabilization ("stabilizing plate") (Fig.1(a)). An example of modified optical layout ("modified" hereafter) has been studied in order improve the co-ECCD capabilities within the existing geometrical constraints, introducing a light cylindrical curvature (R_{cyl} = 0.7 m) of the first mirrors, tilting the fixed mirror by 5° and repositioning the aperture of the stabilizing plate [2].

In the GRASP® environment, the behaviour of the beam propagation inside the antenna can be followed by means of Physical Optics simulations. It is essentially a three steps procedure consisting in the propagation of an electromagnetic field from the source to a structure (tipically a reflector), then the calculation of the induced currents on the reflectors and last the calculation of irradiated field produced by currents induced on the surface plus incident wave. Using geometrical optics the correspondence between mechanical parameters (dz and shaft rotation angle) and launching data (toroidal and poloidal angles) has been mapped for both layouts and both frequencies; Figure 1(b) shows, for the baseline case, the toroidal and poloidal angles as a function of shaft rotation angle and mirror dz movement, for both waveguides. The injection angles and the launching points are used as input in physical performances simulations (see below).
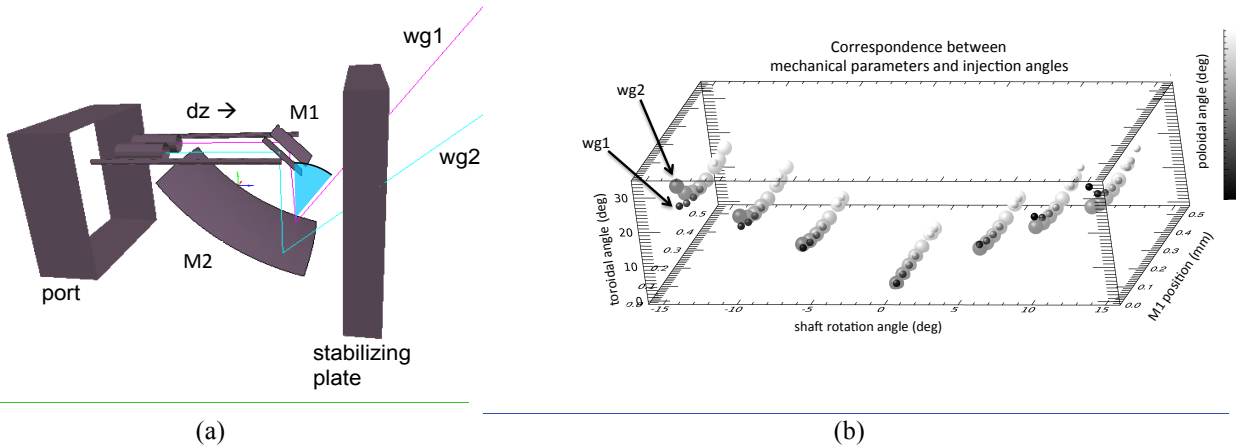
(a)   (b)

FIGURE 1. (a) Geometrical model in the GRASP environment; two examples of ray trajectories are shown. The linear movement of the M2 mirrors (dz) induces the poloidal angle variation (colored angle), while their rotation reflects on toroidal rotation. (b) Correspondence between mechanical parameters (shaft rotation angle in degrees and M1 position in mm on x and y axis respectively) and launching data (toroidal and poloidal injection angles) for the baseline layout. Different symbols stand for different waveguides wg_1 (large transparent dots) and wg_2 (small solid dots).

Beam propagation and Optical Performances

For a systematic scanning of the full toroidal θ_{tor}=(0°,25°) and poloidal θ_{pol}=(-40°,20°) angle ranges, the beams have been simulated on rectangular grids placed approximately 3 meters from their respective launching points on M2; the center of the grid corresponds to the central ray trajectory. In Fig. 2(a) a typical example of simulated beam is shown; variations of the contours with toroidal and poloidal angles are observable in Fig. 2(b). Beam quality, spot dimensions and power density have been evaluated over the full steering range and modeled in term of astigmatic gaussian beams for physics analysis.

Real features of the beam are under study, together with possible interaction with the plate, in order to give a realistic desctription as input for ECCD calculations.

The same kind of beam simulations for the tilted modified layout results generally in a change of shape due to a curvature introduced on the flat mirror M1; Fig. 2(c) shows the comparison between the two layouts: the modified case is generally more focused with a higher peak power density.
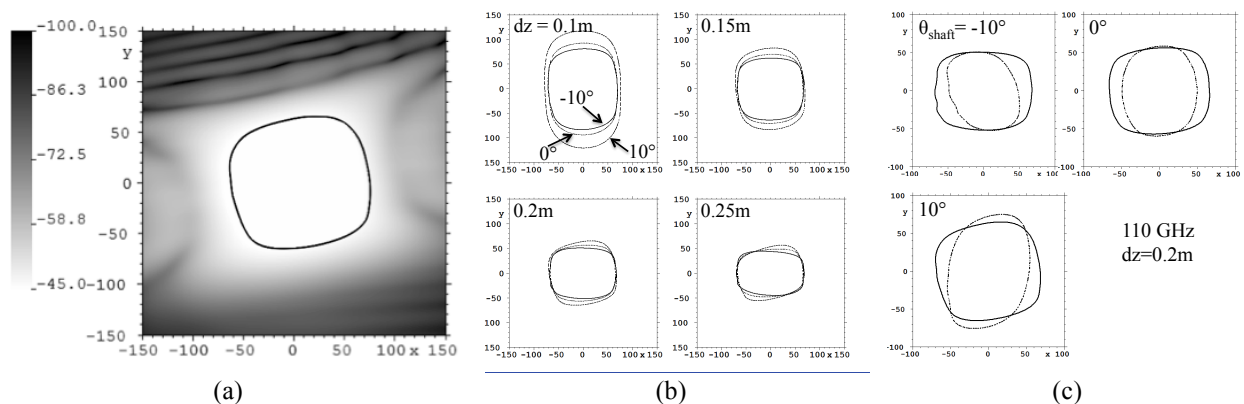

(a)   (b)   (c)

FIGURE 2. (a) An example of 110 GHz simulated beam coming from wg_1 at approximately 3 m from M2 (dz=0.2 m, θ_{shaft}=10°, corresponding to θ_{tor}=24.8°, θ_{tor}=-21.9°); the units of the color palette are arbitrary, the superimposed black contour corresponds to -8.7 dB level from the maximum of the field on the calculation grid. (b) Variation of the -8.7 dB from maximum contours with mechanical parameters for wg_1 at 110 GHz on grids placed ≈ 3m from M2: in each plot dz is fixed and θ_{shaft} varies (solid line = -10°, short dashed = 0°, long dashed = 10°). (c) Comparison between baseline and modified layout beams for wg_1, 110 GHz, dz=0.2 m; each plot shows -8.7 dB from maximum contours (solid for baseline, dashed for modified) at different angles.

ANTENNA PHYSICAL PERFORMANCES FOR INDUCTIVE AND ADVANCED SCENARIOS

The physics performances of the EC system described above have been investigated on the basis of the stationary phase in the current flat top of two plasma scenarios [4]: (i) the full-current I_p = 5.5 MA inductive scenario #2, with a reference magnetic field B_0=2.25 T at a major radius R_0=2.96 m, and central electron density and temperature $n_{e0} = 0.78 \; 10^{20} \; m^{-3}$, $T_{e0} = 12.7 \; keV$, and (ii) the advanced scenario #5-1 with fully non-inductively driven current I_p = 2.3 MA, at B_0=1.72 T with $n_{e0} = 0.68 \; 10^{20} \; m^{-3}$ and $T_{e0} = 5.9 \; keV$. For a wave frequency f = 138 GHz the n-th harmonic cold resonance occurs at a magnetic field $B_{res} \approx (4.9/n)$ T, while for f = 110 GHz the resonant field is B_{res} = (3.9/n) T: to have the second harmonic resonance sufficiently close to the plasma magnetic axis, the higher frequency is more suitable for the scenario #2, and the lower frequency for the scenario #5-1.

The two configurations scenario#2–138 GHz and scenario#5–110 GHz have been selected for the analysis. In each scenario the achievable range in normalized radius ρ (i.e. is the square root of the normalized toroidal flux) and the dependence of the driven current on the injection angles have been assessed through beam-tracing simulations with the code GRAY [3] over a wide interval of the poloidal and toroidal injection angles α = arctan(N_{z0}/N_{R0}) and β = arcsin($N_{\phi0}$), defined here in terms of the cylindrical components of the refraction index vector $\mathbf{N_0}$ at launch.

The full detail of the optical analysis described in the previous section has been used to model the Gaussian beam used for the performance analysis. The general astigmatism induced by the optics has been taken into account, as well as the shift of the reflection point on M2 when the launching angles are varied, and the corresponding changes in the beam spot size and phase front curvature at the launching mirror. The analysis has been repeated both for the baseline optical design and for the modified one with a tilted M2. Figure 3(a) shows the 110 GHz beam trajectory in scenario #5, injected from the waveguide wg_2 in the baseline design. It can be noted that for this scenario the third harmonic resonance is very close to the plasma at the equatorial plane with possible detrimental effects on ECCD efficiency when the beam is aimed at the plasma center.
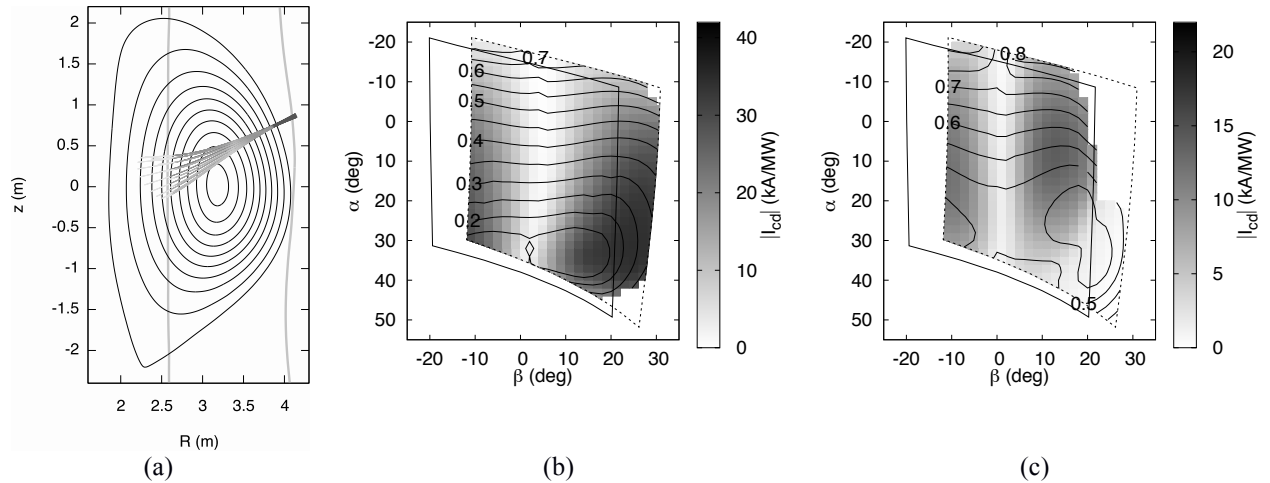

(a)   (b)   (c)

FIGURE 3. (a) 110 GHz beam injection in scenario#5 with α=25º, β=10º. n=2 resonance is on the HFS of the magnetic axis, n=3 is at the LFS plasma edge. (b) Current I_{cd} driven from wg_1 in scenario#2 for f=138 GHz. Black labeled contours show the radial location ρ of the driven current. β>0 delivers co-CD, β<0 cnt-CD. The steering limits are indicated with a polygon for both the baseline design (solid) and the modified one (dashed). (c) Same as (b) for scenario#5 and f=110 GHz.

The amount of current I_{cd} driven in the plasma for a given injection angle has only a weak dependence on the beam shape, so that the results obtained for I_{cd} and shown in Figures 3(b) and 3(c) closely resemble those already obtained in [4], where a stigmatic beam was injected from a fixed point at the center of M2. However, taking into account the details of the optical design allowed an exact estimate of the variations required on the launching angles to compensate the shift of the launching point, and a precise assessment of the limitations on the maximum physics performances due to the optical and mechanical constraints. The results shown here refer to wave injection from the waveguide wg_1, with wg_2 having completely equivalent performance apart from a slight difference in the steering limits due to the toroidal offset in the port with respect to wg_1.

Figures 3(b) shows that in scenario#2 current drive at f = 138 GHz is possible in the range $0.15 \leq \rho \leq 0.7$, with a maximum driven current at a given radius ρ for toroidal injection angles $\beta \geq 20°$, peaking at about Icd ≈ 35 kA/MW at $\rho = 0.2$. The M2 tilt in the modified design is effective in achieving higher co-CD efficiency, raising the upper limit in β from 20° to approximately 30°. Figures 3(c) shows the results for beam injection at f = 110 GHz in scenario#5: the current can be driven in the radial range $0.45 \leq \rho \leq 0.8$, with maximum current $I_{cd} \approx 12$ kA/MW obtained at $\rho = 0.55$ for $\beta = 12°$, and incomplete wave absorption if aiming at $\rho > 0.5$ with $\beta > 20°$. In this case the modified design doesn't carry any significant advantage, except for a small extension of the steering range at large radii, from $\rho = 0.75$ to approximately $\rho = 0.8$. In scenario#5 current drive is not possible at $\rho \leq 0.4$ both because the n=2 resonance lies too far from the magnetic axis and because n=3 resonance limits CD efficiency when aiming at the plasma center, with only 40% of the injected power available at n=2.

In scenario#2, the current density profile width w_{cd} has a weak dependence both on β and ρ for $\beta \leq 18°$, staying almost constant at $w_{cd} \approx 0.07$ m over the range $0.2 \leq \rho \leq 0.7$, so that β can be pushed to values close to 20° to increase I_{cd} maintaining a narrow profile. However, Figure 4(a) shows that the profile broadens quickly if β is increased further (only possible with the modified design). On the contrary, Figure 4(b) shows that in scenario#5 the dependence on β is strong already at lower values: the current profile width increases from $w_{cd} \approx 0.08$ m at $\beta = 10°$, where the peak current density is maximized, up to $w_{cd} \approx 0.20$ m at $\beta = 18°$. Low β values angles are thus to be preferred if well localized CD is required. The changes in current density profile width w_{cd} due to the modifications in the optical design are small but positive, with a reduction of w_{cd} of about 5-10% at the outer radii.
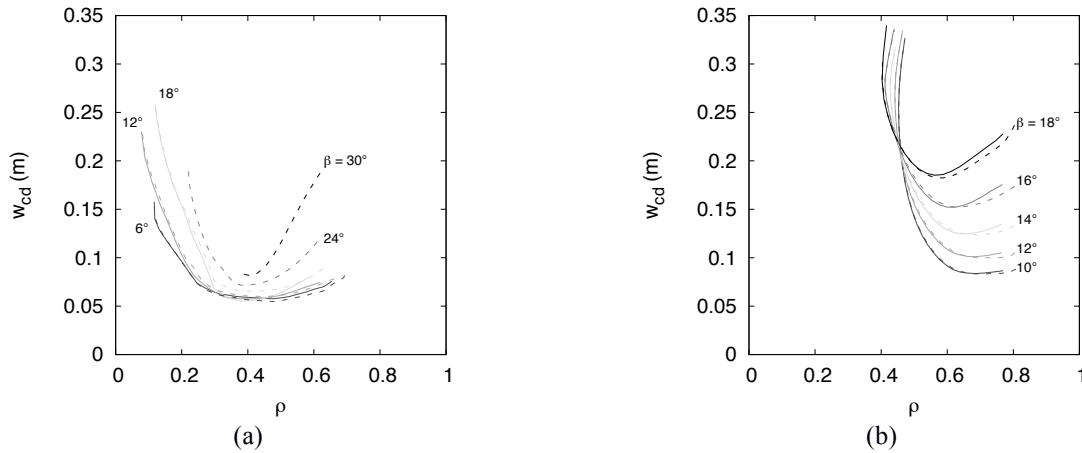

FIGURE 4. (a) Current density profile width in scenario#2 at f=138 GHz for different toroidal launching angles with the baseline (solid) and modified (dashed) optical design. (b) Same as (a) for scenario#5 at f=110 GHz.

ACKNOWLEDGMENTS

REFERENCES

1. T. Kobayashi, S. Moriyama, T. Fujiii, K Takahashi, K. Kajiwara and K. Sakamoto, Fusion Eng. and Des. **84**, 1063-1067 (2009).
2. T. Kobayashi, et al., Mechanical and quasi-optical design of ECH/ECCD launcher for JT-60SA, Proceedings of 28th Symposium on Fusion Technology (SOFT2014), San Sebastián, Spain, to be published in Fusion Eng. and Des. (2015). (doi: 10.1016/j.fusengdes.2015.02.036)
3. D. Farina, Fusion Sci. Technol. , (2007).
4. JT-60SA Research Plan - Research Objectives and Strategy Version 3.2 2015, February, www.jt60sa.org/pdfs/JT-60SA_Res_Plan.pdf.